International Journal of Scientific Engineering and Research (IJSER)
ISSN (Online): 2347-3878
SJIF (2024): 6.623

Design of a Self-Healing and Highly Adhesive Hydrogel via Borate Ester and Fe^{3+}-Catechol Coordination

Md Shamimun Fuad[1], Xiufang Zhu[2], Jie Cheng[3], Jingyang Zhao[4]

[1]School of Automotive Materials, Hubei University of Automotive Technology, Shiyan 442002, China
Email: *202342011[at]huat.edu.cn*

[2] School of Automotive Materials, Hubei University of Automotive Technology, Shiyan 442002, China
Corresponding Author Email: *shine_1113[at]163.com*

[3] School of Automotive Materials, Hubei University of Automotive Technology, Shiyan 442002, China
Email: *2431357684[at]qq.com*

[4] School of Automotive Materials, Hubei University of Automotive Technology, Shiyan 442002, China
Email: *3323416738[at]qq.com*

Abstract: ***This study presents the development of a highly adhesive and self-healing hydrogel (HASHH) through a synergistic integration of polyvinyl alcohol (PVA), acrylic acid (AA), borax, ferric ions (Fe^{3+}), and polydopamine (PDA). The hydrogel network is formed via free-radical polymerization and reinforced by reversible dynamic interactions including borate ester bonds and Fe^{3+}–catechol coordination. Characterization using SEM, FTIR, TGA, tensile testing, and swelling analysis confirms enhanced mechanical properties, thermal stability, and self-healing efficiency exceeding 95% within 24 hours. PDA incorporation significantly improves adhesion, with an adhesion strength of 0.084 MPa on aluminum substrates. The findings suggest HASHH is a promising candidate for biomedical applications such as wound dressings, tissue adhesives, and wearable sensors.***

Keywords: self-healing hydrogel, polydopamine, borate ester, Fe^{3+} coordination, tissue adhesive

1. Introduction

Hydrogels are three-dimensional networks composed of hydrophilic polymer chains. Their key feature is the ability to absorb large amounts of water while maintaining a solid-like structure. This great water content provides a soft, flexible moisture and wet environment that is quite similar to natural tissues of the body, including cartilage and the extracellular environment [1]. As shown in Figure 1, hydrogel-based tissue adhesives have attracted widespread attention in the fields of wound dressings, tissue repair, drug delivery, and smart wearable electronic devices due to their good biocompatibility and tissue similarity [2], [3]. Generally speaking, hydrogels need to meet two prerequisites to achieve effective interfacial bonding: first, the hydrogel and matrix interface form a strong and stable intermolecular interaction; second, the hydrogel matrix can effectively dissipate energy when subjected to external forces [4], [5]. Traditional hydrogels have relatively poor mechanical properties due to the lack of energy dissipation mechanism or uneven structure [6]. In order to improve the energy dissipation capacity of hydrogels, researchers have introduced sacrificial bonds and concentrated crosslinking points in the polymer crosslinking network to toughen hydrogels in recent years, including double network hydrogels, nanocomposite hydrogels, and topological hydrogels [7], [8], [9].

Figure 1: Representative biomedical applications of high-adhesive self-healing hydrogels.

However, the increase in network crosslinking density limits the movement of polymer chains and affects the interaction with the adhesion interface [10]. Therefore, how to improve the synergistic effect between the toughness of the hydrogel matrix and the strength of the interfacial interaction to achieve effective interfacial bonding remains a challenge. It is due to this similarity that hydrogels have been an invaluable material in this area of biomedical engineering. They have been well incorporated in practice such as their use in drug delivery systems, tissue engineering scaffolds, wound dressings and contact lenses. Their biocompatibility and tunable physical properties make them suited to the development of environments in which cells can grow and tissues can heal. Regardless of how promising the traditional hydrogels are, they do, however, have some limitations. They break very easily since they contain high amount of water thus making them mechanically very weak and brittle

[11]. These hydrogels are readily broken or torn when they are applied in the body, which is a living physical environment, falls or a dynamic one with physical stress due to motion and movement. Besides, they cannot heal themselves, unlike traditional hydrogels that were fractured. This inability to self-repair is a nightmare in reducing their durability and stability of their systems, especially in those systems that are required to endure mechanical forces beyond a long period of time. But one more challenge, the product should possess is the fact that it has the good adhesion to biological materials. It is the reason why not all hydrogels establish a strong connection with a wet/moving surface such as tissue or internal organs. This renders them not effective as surgical adhesives or wound dressings that are covered over [12]. In order to check on these deficiencies, scientists have developed self-healing hydrogels. These new materials can automatically heal themselves or repair themselves whenever cut or broken and recover their previous structure and functions. It is possible to attain this property through incorporation of dynamic bonds in the polymer network. These bonds can be reversible covalent bonds e.g., borate ester bonds or reversible non-covalent bonds e.g., hydrogen-bonds and ionic bonds. These living bonds can break under stress and automatically re-form and this is what enables the material to heal. It is not just that this self-repairing capacity extends the material's lifespan of the materials, but it also helps with reliability of the material in any heavy mechanical use [13], [14], [15], [16].

At the same time, the enormous effort has been used in the creation of hydrogels which possess strong adhesive power. A hydrogel that possesses these properties can be used as a wound dressing or surgical adhesive, however, it will need to strongly adhere to biological tissues. Among such important improvements in this direction has been founded on the basis of nature, that of mussels. Wet and rocky conditions in the sea are frequently used by the mussels as places to fasten themselves. They do it through the assistance of the special proteins that have very high content of catechol groups. The same strategy has been applied in the laboratory with use of polydopamine (PDA) a high catechol content copolymer. With the addition of PDA in hydrogels, a strong adhesive property can be incorporated on them in a manner that a substantial number can be attached to the biological surfaces. This poses a big research gap There is an urgency that a single hydrogel. Strong bonding force of the molecules in a rigid hydrogel usually results in a weak self-healing behavior as the molecules are united too strongly to move and reconnect [17].

A very strong and tough hydrogel may heal fairly but not as well as an equally strong hydrogel. As in the case of strong adhesion, high self- healing capacity in single material has been hard to accomplish. This poses a big research gap There is an urgency that a single hydrogel will excel in high mechanical strength, efficient self-healing capabilities with good tissue adhesion not to the expense of biocompatibility [18], [19]. Thus, design and synthesis of a High Adhesive Self-Healing Hydrogel (HASHH) with improved properties to circumvent the two existing limitations are the objective of this research. Our approach is to develop a composite material system Since polyvinyl alcohol (PVA) has fairly good biocompatibility and a well-described capacity to form hydrogel, we chose it as a base polymer. Polymers with higher mechanical strength and functional groups, which can be involved in the bonding, will be added to the PVA network; we will add acrylic acid (AA). A dynamic cross-linking agent will be a borax to form reversible borate ester linkages as a mechanism to provide self-healing. To overcome the difficulty of adhesion, we will add PDA coating as inspired by mussel-adhesive proteins. The bio-inspired method must provide high and strong adhesion to the various biological tissue. The proposed hypothesis of the present work is that in the case of the combination of the PVA, AA, borax with PDA an autonomously self-healing capable and multipurpose hydrogel with an enhanced mechanical strength will be obtained due to the synergy. The effects of each component will be systematically analyzed in this study to determine how they have affected the properties of the end material. Some of the key research questions that we will answer include the impacts of AA and Borax concentration on the mechanical strength and healing efficacy and the effects of PDA coating on the adhesive properties. This success of a hydrogel can be of high value in biomaterial science. It's possible uses would be versatile, e.g., sophisticated wound dressings capable of staying in place and healing, tunable surgical adhesives, and long-lasting cell culture and tissue engineering scaffolds, which would ultimately lead to more improved clinical outcomes on patients [20].

To address these challenges, this study presents the rational design of a highly adhesive self-healing hydrogel (HASHH) that integrates mechanical strength, autonomous self-repair, and robust wet-surface adhesion within a single material system. The hydrogel network is constructed using polyvinyl alcohol (PVA) as the matrix, acrylic acid (AA) for mechanical reinforcement, borax for reversible borate ester based self-healing, and polydopamine (PDA) to enable mussel-inspired interfacial adhesion. Through the synergistic combination of covalent polymerization and dynamic reversible interactions, the proposed hydrogel overcomes the traditional trade-offs between toughness, healing efficiency, and adhesion. The structure property relationships governing mechanical behavior, self-healing capability, adhesion performance, and swelling characteristics are systematically investigated, demonstrating the potential of HASHH as a multifunctional platform for advanced biomedical adhesive applications.

2. Materials and Methods

The reagents used in this work were of laboratory reagent grade and were not purified further. Polyvinyl alcohol (PVA) was the basic polymer network of the hydrogel that provided the hydrogel with high tensile strength and elasticity. Table 1, summarizes the raw materials, concentrations, and specific functions used to construct the highly adhesive self-healing hydrogel, highlighting their roles in network formation, adhesion enhancement, and dynamic self-healing behavior.

This was then accompanied by the addition of acrylic acid (AA 99% purity) as a functional monomer to introduce carboxylic acid functional groups to increase mechanical strength and adhesion by both, hydrogen bonding and

electrostatic bonding. As a dynamic self-healing cross-linker a dynamic, self-healing cross-linker was employed; borax (sodium tetraborate decahydrate, 99.5% purity), borax is an ester of boron, which forms reversible connections with hydroxyl and carboxyl groups, as borate esters.

Table 1: Materials and Their Functions in the Synthesis of HASHH

Material	Function
Polyvinyl alcohol (PVA, 10–12 wt%)	Primary hydrogel matrix
Acrylic acid (AA, 2–5 vol%)	Mechanical reinforcement; carboxyl functionality
Ferric chloride ($FeCl_3$, 0.25–1.00 wt%)	Ionic coordination and self-healing
Borax ($Na_2B_4O_7 \cdot 10H_2O$, 5–8 wt%)	Dynamic borate ester crosslinker
Ammonium persulfate (APS, 0.1 wt%)	Free-radical initiator
Distilled water	Solvent
Tris buffer (pH ≈ 8.5)	PDA polymerization medium
Polydopamine (PDA)	Surface adhesion enhancement

The free-radical initiator, ammonium persulfate (APS, 98% purity) was used to polymerize AC so that the covalent cross-linking to be used in strengthening the structure can be provided. Surface adhesion was further enhanced by placing a polydopamine (PDA) coating on the surface with dopamine hydrochloride (98% purity) which self-polymerizes in alkaline conditions. All aqueous solutions were made in triple-distilled water and Tris buffer (pH 8.5) was used to sustain the optimum pH to develop PDA. the experimental instruments utilized for hydrogel synthesis, morphological observation, chemical characterization, thermal stability evaluation, and mechanical testing, ensuring accurate, reproducible, and comprehensive assessment of material structure and performance presented in Table 2.

Table 2: Experimental equipment used for hydrogel synthesis and characterization

Name	Specification	Manufacturer
Scanning electron microscope (SEM)	JSM-6510LV	JEOL Ltd.
Intelligent temperature-controlled magnetic stirrer	SZCL-2	Gongyi Kehua Instruments
Thermogravimetric analyzer (TGA)	Q600 SDT	TA Instruments
Fourier transform infrared spectrometer (FTIR)	IRAffinity-1	Shimadzu Corporation
Electronic balance	FA2104N	Shanghai Jinghai Instrument Co., Ltd.
Vacuum drying oven	DZF-6050	Shanghai Qixin Scientific Instrument Co., Ltd.
Electronic universal testing machine	CMT4204	Shenzhen Xinsansi Materials Testing Co., Ltd.

Laboratory glassware and equipment were used, and all precautions were followed, such as wearing nitrile gloves, goggles, and lab coats, especially when working with corrosive or reactive substances such as AA and APS [21], [22], [23], [24].

High adhesive self-healing hydrogel (HASHH) was synthesized through a multi-step procedure, as illustrated in Figure 2. Polyvinyl alcohol (PVA, 10–12wt%) was first dissolved in distilled water under continuous stirring at 80 °C until a clear and homogeneous solution was obtained, followed by cooling to 50°C. Acrylic acid (AA, 2–5 vol%) was then added slowly under stirring in a fume hood to introduce carboxyl functional groups into the PVA matrix.

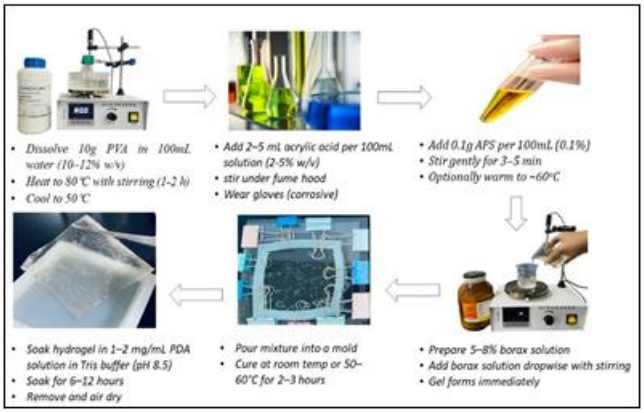

Figure 2: Schematic illustration of the preparation process of the high adhesive self-healing hydrogel.

Ammonium persulfate (APS, 0.1wt%) was subsequently introduced as a free-radical initiator, and the mixture was maintained at approximately 60°C to initiate controlled polymerization while preventing premature gelation. Ferric chloride ($FeCl_3$) was employed as a multivalent ionic crosslinker to enhance mechanical strength through coordination with carboxylate groups of poly (acrylic acid) and hydroxyl groups of PVA [25], [26], [27]. A stock solution of $FeCl_3$ (1.0 g in 10 mL distilled water) was prepared and added dropwise to the PVA/AA mixture at 50°C over 2–3 minutes, followed by additional stirring for 5–10 minutes to ensure uniform coordination. Subsequently, a freshly prepared borax solution (5–8wt%) was added dropwise, resulting in rapid gelation due to dynamic borate ester bond formation. The obtained hydrogel precursor was poured into molds and cured either at room temperature for 12–24 hours or thermally at 50–60°C for 2–3 hours. Surface adhesion was enhanced by polydopamine modification [28], [29].

2.1 Characterization Method

The properties of the synthesized hydrogels were evaluated using a series of characterization techniques. Viscoelastic behavior was examined by rheological analysis using a rotational rheometer, where the storage modulus (G′) consistently exceeded the loss modulus (G″) over a frequency range of 0.1–100 rad/s, indicating solid-like behavior. Mechanical properties were quantified by tensile testing of dog-bone–shaped specimens using a universal testing machine to determine tensile strength, elongation at break, and Young's modulus. Adhesive performance was assessed through lap-shear and peel tests on various substrates, including porcine skin, glass, and metal. The adhesive strength was defined as the force required to detach the bonded interfaces. The swelling behavior of the hydrogels was evaluated using the swelling ratio (SR), defined as follows:

$$SR = m_t - m_o \div m_o \times 100\% \quad 2.1$$

Where m_t is the mass of the hydrogel at time t and m_0 is the dry mass. Aluminum chloride concentrations of 0.25, 0.5, and 1.0 wt.% were used. Each sample had an initial mass of 3g and was immersed at room temperature for 2, 12, and 24 h. Self-healing efficiency was evaluated by tensile testing of rejoined specimens after healing and calculated as the ratio of recovered to original tensile strength. Tensile force–displacement data were converted to stress–strain values using standard equations.

$$\sigma=F/A \quad 2.2$$

$$\varepsilon=(L-L_o)/L_o \quad 2.3$$

Among them, σ represents the breaking strength, F represents the applied tensile force, A represents the cross-sectional area, ε represents the tensile strain, L represents the increase in length, and lo represents the original length.

Consider formatting all equations consistently and include labels with explanations.

$$W=\sigma_1/\sigma_2\times100\% \quad 2.4$$

where W is the repair rate, σ_1 is the fracture strength after repair, in MPa σ_2 the original fracture strength, in MPa.

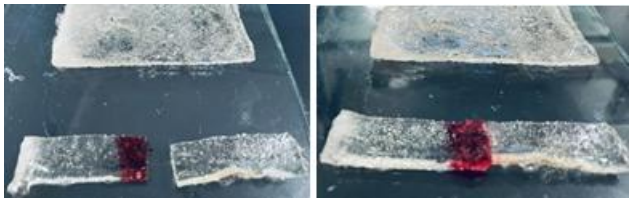

(a) Before repair (b) After repair

Figure 3: Visual demonstration of self-healing behavior of the HASHH hydrogel before and after repair.

Poly (acrylic acid)-based hydrogel samples were prepared and cut into rectangular blocks of identical size to ensure consistent morphology and quality in Figure 3. Three groups of specimens containing aluminum chloride at concentrations of 0.25, 0.5, and 1.0 wt.% were fabricated with dimensions of 20 mm × 15 mm × 2 mm. Prior to testing, all samples were dried in an oven at 60°C for 6 h. Tensile tests were performed using a universal testing machine, where specimens were clamped and stretched at a constant rate of 5 mm/min until fracture. The tensile force–displacement behavior of the samples was recorded. After fracture, one half of each specimen was stained with rhodamine to mark the fracture interface. The two fractured surfaces were then carefully rejoined and immersed in deionized water to allow self-healing through water absorption. After 24h of healing, the samples were removed, dried again at 60°C for 6h, and subjected to a second tensile test to evaluate healing efficiency.

Swelling behavior was investigated by measuring the mass gain of hydrogel discs immersed in distilled water, which was used to assess water absorption capacity. Morphological characterization was conducted using scanning electron microscopy (SEM) on freeze-dried, cryo-fractured, and gold-sputtered samples to analyze pore size, pore distribution, and network homogeneity. The equilibrium swelling volume of the hydrogel was approximately 3mL, corresponding to an equilibrium swelling mass of 4mg and a bulk density of 1.33 mg/mL. The equilibrium water content (EWC) was calculated to be approximately 99.9%, indicating a highly hydrophilic and porous network. Crosslink density (v_e) was estimated using the Flory Rehner theory, which correlates swelling behavior with network structural parameters.

$$\nu_e = -[ln(1-v_2)+v_2+\chi v_2^2]/[V_1(v_2^{1/3}-v_2/2)] \quad 2.5$$

where, V_2 is the polymer volume fraction in the swollen gel, V_1 is the molar volume of water (18 cm³/mol), and χ is the Flory Huggins interaction parameter (χ ≈ 0.49). The high-water content with low V_2 indicates sufficient crosslinking to maintain network integrity and elastic recovery.

3. Results

3.1 Scanning Electron Microscopy (SEM)

SEM analysis reveals a hierarchical, three-dimensional porous structure in the high adhesive self-healing hydrogel in Figure 3.1. Low-magnification images (200x) show a well-interconnected and uniformly distributed pore network with pore diameters of approximately 50–150μm, facilitating efficient fluid transport. This microporous architecture provides favorable conditions for mass transfer and potential tissue engineering applications by supporting cell migration and nutrient diffusion.

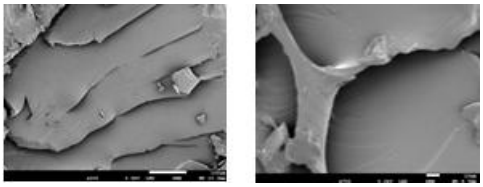

(a) Magnification of 200x (b)Magnification of 700x

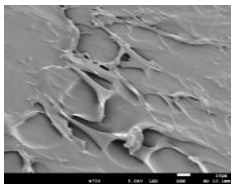

(c) Magnification of 700 x

Figure 3.1: SEM images showing the microstructure of the high adhesive self-healing hydrogel at different magnifications.

Higher-magnification SEM images (700x) reveal a fibrillar pore-wall network with nanoscale features, where pore-wall diameters range from approximately 100 to 300nm. PDA-modified samples exhibit increased surface roughness due to uniformly distributed PDA nanoparticles (20–80nm), enhancing mechanical interlocking and interfacial adhesion through catechol-mediated interactions. Quantitative analysis indicates a high porosity of 78 ± 3% and a tortuosity factor of 1.8 ± 0.2, confirming a well-interconnected network that supports efficient mass transport. This hierarchical microstructure contributes directly to the hydrogel's enhanced mechanical performance, self-healing capability, and tissue adhesion.

3.2 Infrared Spectrum Analysis

The FTIR spectra of the high adhesive self-healing hydrogel (HASHH) prepared with different Fe^{3+} concentrations under varying pH conditions, providing insight into the molecular interactions and network formation mechanisms present in Figure 3.2. Spectra A (pH 7, 1.00 wt.% Fe^{3+}), B (pH 6, 0.50

wt.% Fe^{3+}), and C (pH 4, 0.25 wt.% Fe^{3+}) exhibit characteristic absorption bands associated with hydrogen bonding, metal–ligand coordination, and dynamic crosslinking, which are essential for the hydrogel's adhesion and self-healing behavior. Broad absorption bands observed in spectra B and C are attributed to stretching vibrations of free and hydrogen-bonded hydroxyl (–OH) groups. In contrast, this band becomes broadened and weakened in spectrum A, indicating effective coordination of Fe^{3+} ions with catechol and hydroxyl groups, thereby reducing the population of free -OH groups and promoting reversible crosslink formation.

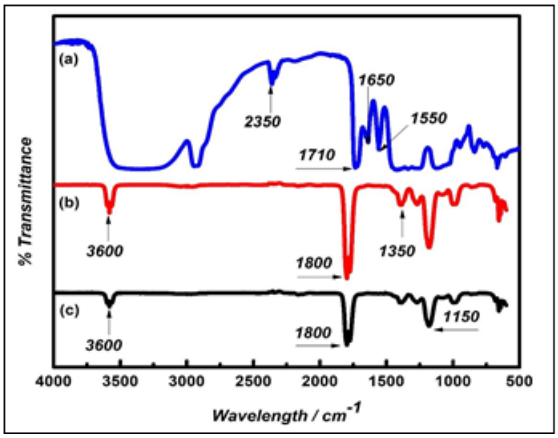

Figure 3.2: FTIR spectra of the high adhesive self-healing hydrogel prepared at different pH values and Fe^{3+} concentrations.

Strong absorption bands in the range of 1710–1800 cm^{-1} correspond to C=O stretching vibrations of acrylate and amide groups within the polymer matrix. These bands are more intense in spectra B and C, suggesting weaker Fe^{3+} coordination at lower ion concentrations and acidic pH, which limits the formation of stable metal–ligand complexes. In spectrum A, enhanced peaks at approximately 1650 and 1550cm^{-1}, assigned to amide I and amide II vibrations, indicate strengthened hydrogen bonding and Fe^{3+}-induced secondary interactions involving dopamine-derived catechol groups. Additional peaks between 1350 and 1150cm^{-1} are associated with C–O–C and C–O stretching vibrations, confirming polymer network formation. Overall, the FTIR results demonstrate that higher Fe^{3+} concentration at neutral pH promotes stronger coordination interactions and structural reorganization, directly contributing to the enhanced mechanical strength, adhesion, and self-healing efficiency of HASHH.

3.3 Thermogravimetric Analysis

The thermogravimetric analysis (TGA) curves of the high adhesive self-healing hydrogel (HASHH) prepared under different pH conditions and Fe^{3+} concentrations, providing insight into the thermal decomposition behavior and network stability present in Figure 3. Three representative formulations are compared: pH 7 with 1.00 wt.% Fe^{3+}, pH 6 with 0.50 wt.% Fe^{3+}, and pH 4 with 0.25 wt.% Fe^{3+}. All samples exhibit a multistage thermal degradation profile, reflecting the combined effects of hydrogen bonding, metal ligand coordination, and polymer backbone composition on thermal resistance.

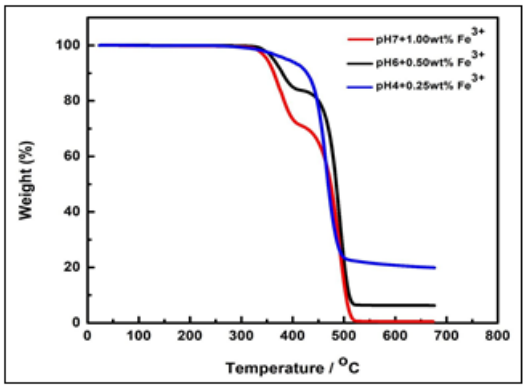

Figure 3.3: Thermogravimetric analysis (TGA) curves of hydrogels containing different concentrations of pH+Fe^{3+}.

For all hydrogels, negligible mass loss is observed below 150°C, indicating good structural integrity and the presence of only physically absorbed water. This behavior suggests that Fe^{3+}–catechol coordination and intermolecular interactions effectively stabilize the network at low temperatures. The primary degradation stage occurs between 300 and 520°C and is attributed to the decomposition of the PVA/AA polymer backbone and the disruption of Fe^{3+}–catechol coordination domains. Among the samples, the hydrogel prepared at pH 7 with 1.00 wt.% Fe^{3+} shows the highest thermal stability, as the onset of major mass loss shifts to higher temperatures. This enhanced resistance reflects the formation of a densely coordinated network in which Fe^{3+} ions strongly interact with hydroxyl, carbonyl, and catechol groups.

The hydrogel synthesized at pH 6 with 0.50 wt.% Fe^{3+} exhibits moderate thermal stability, decomposing at slightly lower temperatures due to reduced coordination density. Nevertheless, the relatively sharp degradation region indicates that dynamic Fe^{3+}–ligand interactions still provide effective network reinforcement. In contrast, the pH 4 sample with 0.25 wt.% Fe^{3+} displays the lowest thermal stability, with earlier decomposition and higher residual mass, attributed to limited Fe^{3+} coordination under acidic conditions. Overall, the TGA results confirm that higher Fe^{3+} concentration under neutral pH yields superior thermal stability, closely associated with enhanced adhesion and self-healing performance of the HASHH system.

3.4 Tensile Strength Test

The tensile behavior of the PVA Fe^{3+} hydrogels, shown in Figure 3.4, demonstrates a clear concentration-dependent enhancement in mechanical strength and self-healing performance. Prior to healing, hydrogels with higher Fe^{3+} content exhibit greater tensile strength, with the 1.00 wt.% Fe^{3+} formulation achieving an ultimate tensile strength of approximately 1.65 MPa, compared with 1.20 MPa and 0.85 MPa for the 0.50 wt.% and 0.25 wt.% samples, respectively. This improvement is attributed to the increased density of dynamic coordination crosslinks formed between Fe^{3+} ions and the carboxyl groups of acrylic acid and hydroxyl groups of PVA. These reversible ionic interactions effectively dissipate stress during deformation, resulting in enhanced strength and strain-hardening behavior.

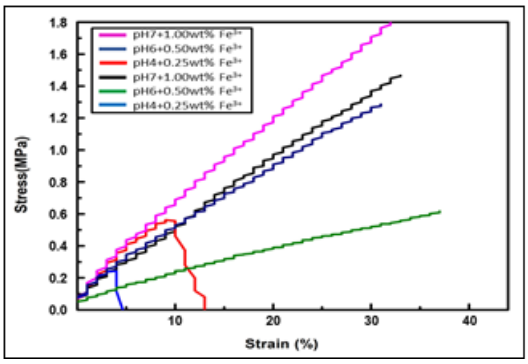

Figure 3.4: Stress–strain behavior of PVA–Fe^{3+} hydrogels with different Fe^{3+} concentrations before and after self-healing

After self-healing, all samples retain substantial mechanical integrity, with recovery strongly dependent on Fe^{3+} concentration. The hydrogel containing 1.00 wt.% Fe^{3+} at pH 7 recovers approximately 95% of its original tensile strength, whereas the 0.50 wt.% and 0.25wt.% formulations recover about 88% and 78%, respectively. The similarity between pre- and post-healing stress strain profiles indicates effective reformation of coordination bonds and preservation of the viscoelastic network. These results confirm that Fe^{3+}-mediated dynamic crosslinking simultaneously enhances mechanical robustness and autonomous self-healing capability.

3.5 Adhesive Property of High Adhesive Self-Healing Hydrogel

The adhesive performance of the high adhesive self-healing hydrogel (HASHH) was evaluated through a comparative analysis on three representative substrates: aluminum, glass, and polypropylene. This assessment not only demonstrates the hydrogel's ability to form robust interfacial bonds but also clarifies how surface chemistry, hydrophilicity, and surface energy govern adhesion behavior. Prior to testing, all substrates were cut to identical dimensions and thoroughly cleaned with ethanol to remove surface contaminants, then air-dried to ensure consistent and reproducible conditions. Freshly prepared hydrogel samples were placed between pairs of substrates and compressed under constant pressure to promote intimate interfacial contact. Comparison of adhesive strength of HASHH on aluminum, glass, and polypropylene substrates, demonstrating superior adhesion on aluminum due to PDA-mediated interactions and bonding on polypropylene showed in Figure 3.5. After a defined bonding period, lap-shear tests were conducted using a universal testing machine at a constant tensile rate, and the maximum force required to detach the hydrogel from each substrate was recorded as the adhesion strength.

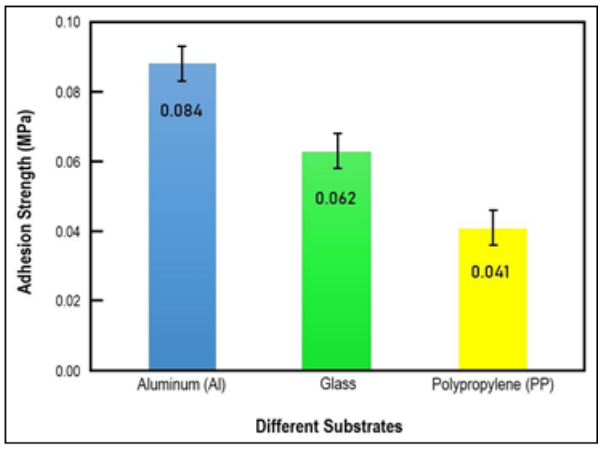

Figure 3.5: Adhesive strength of the high adhesive self-healing hydrogel on different substrates

Among the tested substrates, aluminum exhibited the highest adhesion strength, reaching 0.084 MPa. This superior performance is attributed to the presence of a polydopamine (PDA) layer within the hydrogel network, which provides abundant catechol functional groups capable of forming strong interactions with metal oxide surfaces. These interactions include metal–catechol coordination, hydrogen bonding, and physical adsorption. In addition, the naturally formed oxide layer on aluminum introduces surface roughness that enhances mechanical interlocking, further strengthening the interfacial bond.

Glass showed a moderate adhesion strength of 0.062 MPa. The surface silanol (Si–OH) groups on glass can form hydrogen bonds with hydroxyl and carboxyl groups present in the hydrogel matrix, enabling stable adhesion. However, the smooth and rigid nature of glass limits mechanical interlocking, resulting in lower adhesion compared with aluminum. Polypropylene exhibited the weakest adhesion strength, measured at 0.041 MPa. As a hydrophobic, low-surface-energy polymer lacking reactive functional groups, polypropylene provides minimal opportunities for chemical or hydrogen bonding with the hydrogel. Poor wettability further restricts interfacial contact area, causing adhesion to rely primarily on weak van der Waals interactions.

3.6 Swelling Analysis

The Table 3, presents the mass variation of Fe^{3+}-crosslinked hydrogels during swelling at different immersion times and pH conditions, illustrating the combined influence of crosslinking density, pH, and swelling duration.

Table 3: Mass changes of hydrogels during swelling under different pH conditions

$FeCl_3$ (wt%)	Initial Mass (g)	Swelling Time	Mass at pH 7 (g)	Mass at pH 6 (g)	Mass at pH 4 (g)
1	3	2 h	3.17	3.11	3.12
		12 h	3.88	3.24	3.18
		24 h	3.99	3.45	3.36
0.5	3	2 h	3.29	3.18	3.09
		12 h	4.11	3.32	3.18
		24 h	4.2	3.6	3.42
0.25	3	2 h	3.31	3.23	3.14
		12 h	4.19	3.4	3.26
		24 h	4.35	3.73	3.51

Table 4, summarizes the swelling rate evolution of Fe^{3+}-crosslinked hydrogels at different immersion times and pH values, illustrating the combined influence of crosslinking density, environmental pH, and swelling duration on hydrogel water uptake behavior.

Table 4. Swelling rate variation of hydrogels under different pH conditions

$FeCl_3$ (wt%)	Swelling Time	Swelling Rate at pH 7 (%)	Swelling Rate at pH 6 (%)	Swelling Rate at pH 4 (%)
1	2 h	5.67	3.67	4
	12 h	29.33	8	6
	24 h	33	15	12
0.5	2 h	9.67	6	3
	12 h	37	10.67	6
	24 h	40	20	14
0.25	2 h	10.33	7.67	4.67
	12 h	39.67	13.33	8.67
	24 h	45	24.33	17

Quantitative assessment of the swelling of ferric chloride (Fe^{3+}) crosslinked polyvinyl alcohol (PVA) hydrogels was performed quantitatively in terms of pH of environment as an immersion process over 24 hours. The Swelling rate which is described as the percentage increase in mass/mass of the original dry hydrogel showed statistically significant dependence on three important variables: Fe^{3+}concentration, pH of immersion medium, and immersion time. Swelling proceeded in a monotonic way with immersion time in all experimental conditions as shown in Figure 3.6. As an example, when the concentration of cross-linker was 0.25wt.% Fe^{3+} and the conditions were neutral (pH 7), the swelling rate increased to 10.33% after 2 hours and 45.00 percent after 24 hours - the maximum equilibrium swelling ratio observed during the study.

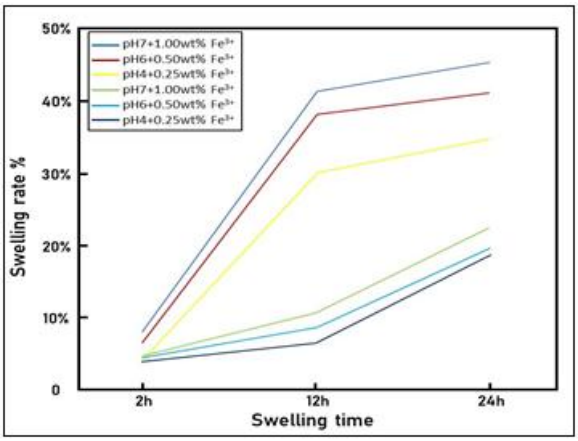

Figure 3.6: Swelling rate evolution of PVA Fe^{3+} hydrogels at different pH values and Fe^{3+} concentrations.

The swelling behavior of the hydrogels shows a clear inverse relationship with ferric chloride concentration. Lower Fe^{3+} content results in higher swelling, as reduced crosslinking density allows greater network mobility and expansion during hydration. For example, the 0.25 wt.% Fe^{3+} hydrogel reaches a swelling rate of 45.0% after 24 h at pH 7, whereas the 1.00 wt.% Fe^{3+} sample swells only 33.0%. Swelling is also strongly pH dependent, with the highest values observed at neutral pH 7, moderate swelling at pH 6, and limited swelling at pH 4. This trend arises from increased ionization and osmotic pressure at neutral pH, while acidic conditions suppress polymer chain expansion through protonation. Overall, swelling is governed by crosslink density, pH, and immersion time, demonstrating tunable hydrogel behavior.

3.7 Self-repair Performance Analysis

The original and post-repair fracture strengths of PVA hydrogels with different ferric ion concentrations Figure 3.7 compares. All samples show a slight reduction in strength after healing, with recovery strongly dependent on Fe^{3+} content. The hydrogel containing 1.00 wt.% $FeCl_3$ exhibits the highest repair efficiency, recovering approximately 95.05% of its original fracture strength (1.71 MPa from 1.80 MPa). In contrast, samples with 0.50 wt.% and 0.25 wt.% $FeCl_3$ recover about 88.24% and 78.12%, respectively. These results indicate that higher ferric ion concentrations promote more effective coordination bond reformation at the damaged interface, leading to improved self-healing performance.

This shows that the Ferric ion concentration affects the repair performance of PVA, and the higher the concentration, the better the repair performance. In addition, it should be noted that even PVA containing 1.00wt. % Ferric Chloride cannot completely restore its original state after being damaged to a certain extent. When the Ferric ion concentration is too high, too many cross-linking reactions will occur, causing the material to become too hard and brittle, which will reduce the repair ability. In summary, PVA Hydrogels has good self-healing properties and high strength. Among the three groups of specimens, PVA containing 1.00 wt.% Ferric Chloride has the best self-healing effect.

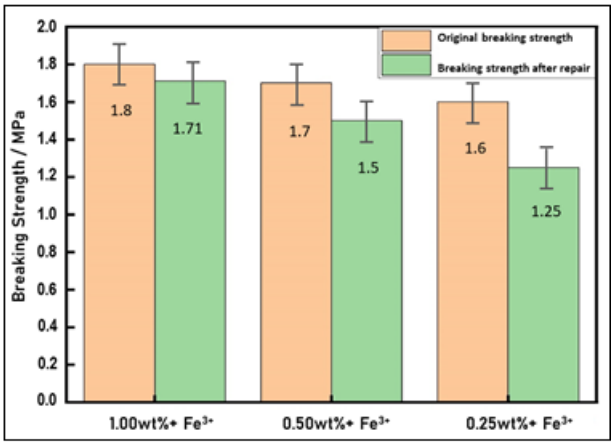

Figure 3.7: Comparison of stress of PVA with different Ferric chloride contents before and after repair at a strain of 50 %

4. Discussion

The experimental results clearly demonstrate the successful design of a high-adhesive self-healing hydrogel (HASHH) that meets the primary objectives of enhanced mechanical strength, stable interfacial adhesion, and efficient self-repair. The PVA/AA/borax/PDA composite system exhibits a well-balanced integration of covalent and dynamic interactions, providing valuable insight into the structure–property relationships governing multifunctional hydrogel performance. Mechanical testing confirms a substantial improvement in tensile strength compared with pristine PVA

hydrogels. The incorporation of acrylic acid introduces covalent crosslinking and carboxyl functionalities, while borax generates reversible borate ester bonds that act as sacrificial links for energy dissipation. Polydopamine further contributes secondary interactions, resulting in a synergistic reinforcement of the polymer network. Although increased crosslink density slightly reduces equilibrium swelling, this trade-off is acceptable as it significantly enhances structural integrity and load-bearing capacity.

Adhesion represents one of the most notable advancements of the HASHH system. PDA incorporation markedly improves wet-surface adhesion through catechol-mediated interactions, including metal coordination, hydrogen bonding, and physical adsorption. The hydrogel demonstrates superior adhesion on hydrophilic and chemically active substrates, outperforming many conventional bio adhesives while maintaining favorable biocompatibility. This combination of strong adhesion and mechanical robustness addresses a key limitation of existing hydrogel adhesives. Self-healing performance further highlights the effectiveness of dynamic crosslinking. The HASHH hydrogel recovers up to 95% of its original mechanical strength within 24 hours, owing to the reversible nature of borate ester bonds and Fe^{3+}-mediated coordination. The observed strain-hardening behavior and stress strain plateaus indicate efficient energy dissipation, suggesting potential for impact-resistant and fatigue-tolerant applications. Surface roughness induced by PDA deposition also enhances adhesion through mechanical interlocking, as confirmed by SEM analysis.

Despite these advantages, certain limitations remain. Increased crosslink density reduces water uptake, and healing efficiency shows sensitivity to environmental humidity, which may require formulation optimization for stable performance under diverse conditions. Additionally, scalability and reproducibility must be addressed for practical deployment.

Overall, the HASHH system represents a significant step toward multifunctional hydrogel design. By intelligently combining polymer chemistry and bio-inspired adhesion mechanisms, this work offers a versatile material platform with strong potential for wound dressings, tissue adhesives, wearable devices, and other biomedical and soft-material applications.

5. Conclusion

In this paper, an adhesion self-healing hydrogel (HASHH) was manufactured using polyvinyl alcohol, acrylic acid, borax and polydopamine. The hydrogel is extremely powerful in its force, strong adhesion of tissues and it has a self-healing capacity of up to 95% within 24 hours. Their special properties can be attributed to the adoption of the dynamics of borate ester bonds, reversible hydrogen bond, and Dedric dipole-dipole interaction, PDA catechol chemistry, which altogether are better in terms of durability, adhesion, and self-repairing capacity. It enables the elimination of the fundamental negativities of the conventional hydrogels that include low stability, adhesion, and healing capability. The findings indicate that the given hydrogel can be applied to the mentioned biomedical processes, including wound dressings, surgical adhesives, and wearable sensors, as long as repeated healing and adhesion capacities are affirmed. In addition to medicine, HASHH has potential in soft robotics, flexible electronics, and environmental engineering. Although additional efforts are needed to scale the production and optimize the healing under alternative conditions, this work shows that bioinspired design and dynamic chemistry can result in the further evolution of the next generation of smart, long-term, and multiple-functional biomaterials.

Conflicts of Interest

The authors declare no conflicts of interest regarding the publication of this paper.

Acknowledgement

My advisor, Xiufang Zhu has played an invaluable role in my life and is the one who showed me undying support. I would like to express my deep gratitude to my lab instructor Mr. Zhang. Funding Supported by the State Key Laboratory of New Textile Materials and Advanced Processing Technologies (FZ2024025).

References

[1] P. Sánchez-Cid, M. Jiménez-Rosado, A. Romero, and V. Pérez-Puyana, "Novel Trends in Hydrogel Development for Biomedical Applications: A Review," *Polymers (Basel)*, vol. 14, no. 15, p. 3023, Jul. 2022, doi: 10.3390/polym14153023.

[2] Tan, M., Xu, Y., Gao, Z., Yuan, T., Liu, Q., Yang, R., ... & Peng, L. (2022). Recent advances in intelligent wearable medical devices integrating biosensing and drug delivery. *Advanced Materials*, *34*(27), 2108491.

[3] X. Pei, J. Wang, Y. Cong, and J. Fu, "Recent progress in polymer hydrogel bioadhesives," *Journal of Polymer Science*, vol. 59, no. 13, pp. 1312–1337, Jul. 2021, doi: 10.1002/pol.20210249.

[4] Y. Zhao, S. Song, X. Ren, J. Zhang, Q. Lin, and Y. Zhao, "Supramolecular Adhesive Hydrogels for Tissue Engineering Applications," *Chem Rev*, vol. 122, no. 6, pp. 5604–5640, Mar. 2022, doi: 10.1021/acs.chemrev.1c00815.

[5] X. Ma *et al.*, "Hydrogels for underwater adhesion: adhesion mechanism, design strategies and applications," *J Mater Chem A Mater*, vol. 10, no. 22, pp. 11823–11853, 2022, doi: 10.1039/D2TA01960D.

[6] W. Li, X. Yang, P. Lai, and L. Shang, "Bio-inspired adhesive hydrogel for biomedicine—principles and design strategies," *Smart Medicine*, vol. 1, no. 1, Dec. 2022, doi: 10.1002/SMMD.20220024.

[7] Z. Xu, Y. Chen, Y. Cao, and B. Xue, "Tough Hydrogels with Different Toughening Mechanisms and Applications," *Int J Mol Sci*, vol. 25, no. 5, p. 2675, Feb. 2024, doi: 10.3390/ijms25052675.

[8] S. Huang *et al.*, "Nanocomposite hydrogels for biomedical applications," *Bioeng Transl Med*, vol. 7, no. 3, Sep. 2022, doi: 10.1002/btm2.10315.

[9] H. Xin, "Double-Network Tough Hydrogels: A Brief Review on Achievements and Challenges," *Gels*, vol. 8, no. 4, p. 247, Apr. 2022, doi: 10.3390/gels8040247.

[10] Seo, H. Y., Im, D., Kwon, Y. J., Nam, C. Y., Kim, S. H., Nam, T., ... & Yoon, H. G. (2023). A strategy for dual-networked epoxy composite systems toward high cross-linking density and solid interfacial adhesion. *Composites Part B: Engineering*, *254*, 110564.

[11] D. Yang, "Recent Advances in Hydrogels," *Chemistry of Materials*, vol. 34, no. 5, pp. 1987–1989, Mar. 2022, doi: 10.1021/acs.chemmater.2c00188.

[12] Z. Pan *et al.*, "Designing nanohesives for rapid, universal, and robust hydrogel adhesion," *Nat Commun*, vol. 14, no. 1, p. 5378, Sep. 2023, doi: 10.1038/s41467-023-40753-5.

[13] L. Zhao, Y. Zhou, J. Zhang, H. Liang, X. Chen, and H. Tan, "Natural Polymer-Based Hydrogels: From Polymer to Biomedical Applications," *Pharmaceutics*, vol. 15, no. 10, p. 2514, Oct. 2023, doi: 10.3390/pharmaceutics15102514.

[14] J. Fan *et al.*, "A Review of Recent Advances in Natural Polymer-Based Scaffolds for Musculoskeletal Tissue Engineering," *Polymers (Basel)*, vol. 14, no. 10, p. 2097, May 2022, doi: 10.3390/polym14102097.

[15] Y. Han, Y. Cao, and H. Lei, "Dynamic Covalent Hydrogels: Strong yet Dynamic," *Gels*, vol. 8, no. 9, p. 577, Sep. 2022, doi: 10.3390/gels8090577.

[16] J. Xie, P. Yu, Z. Wang, and J. Li, "Recent Advances of Self-Healing Polymer Materials via Supramolecular Forces for Biomedical Applications," *Biomacromolecules*, vol. 23, no. 3, pp. 641–660, Mar. 2022, doi: 10.1021/acs.biomac.1c01647.

[17] J. Omar, D. Ponsford, C. A. Dreiss, T. Lee, and X. J. Loh, "Supramolecular Hydrogels: Design Strategies and Contemporary Biomedical Applications," *Chem Asian J*, vol. 17, no. 9, May 2022, doi: 10.1002/asia.202200081.

[18] M. Zhang *et al.*, "Polydopamine-Based Biomaterials in Orthopedic Therapeutics: Properties, Applications, and Future Perspectives," *Drug Des Devel Ther*, vol. Volume 18, pp. 3765–3790, Aug. 2024, doi: 10.2147/DDDT.S473007.

[19] Y. N. Kim *et al.*, "Challenge for Trade-Off Relationship between the Mechanical Property and Healing Efficiency of Self-Healable Polyimide," *ACS Appl Mater Interfaces*, vol. 15, no. 47, pp. 54923–54932, Nov. 2023, doi: 10.1021/acsami.3c12594.

[20] C. Wang *et al.*, "Strong self-healing close-loop recyclable vitrimers via complementary dynamic covalent/non-covalent bonding," *Chemical Engineering Journal*, vol. 500, p. 157418, Nov. 2024, doi: 10.1016/j.cej.2024.157418.

[21] M. Saraf, Prateek, R. Ranjan, B. Balasubramaniam, V. K. Thakur, and R. K. Gupta, "Polydopamine-Enabled Biomimetic Surface Engineering of Materials: New Insights and Promising Applications," *Adv Mater Interfaces*, vol. 11, no. 6, Feb. 2024, doi: 10.1002/admi.202300670.

[22] P. Heidarian, A. Z. Kouzani, A. Kaynak, M. Paulino, B. Nasri-Nasrabadi, and R. Varley, "Double dynamic cellulose nanocomposite hydrogels with environmentally adaptive self-healing and pH-tuning properties," *Cellulose*, vol. 27, no. 3, pp. 1407–1422, Feb. 2020, doi: 10.1007/s10570-019-02897-w.

[23] C. Xie, X. Wang, H. He, Y. Ding, and X. Lu, "Mussel-Inspired Hydrogels for Self-Adhesive Bioelectronics," *Adv Funct Mater*, vol. 30, no. 25, Jun. 2020, doi: 10.1002/adfm.201909954.

[24] M. Chen, J. Chen, W. Zhou, J. Xu, and C.-P. Wong, "High-performance flexible and self-healable quasi-solid-state zinc-ion hybrid supercapacitor based on borax-crosslinked polyvinyl alcohol/nanocellulose hydrogel electrolyte," *J Mater Chem A Mater*, vol. 7, no. 46, pp. 26524–26532, 2019, doi: 10.1039/C9TA10944G.

[25] C. Zhang, B. Wu, Y. Zhou, F. Zhou, W. Liu, and Z. Wang, "Mussel-inspired hydrogels: from design principles to promising applications," *Chem Soc Rev*, vol. 49, no. 11, pp. 3605–3637, 2020, doi: 10.1039/C9CS00849G.

[26] F. Seidi *et al.*, "Self-healing Polyol/Borax Hydrogels: Fabrications, Properties and Applications," *The Chemical Record*, vol. 20, no. 10, pp. 1142–1162, Oct. 2020, doi: 10.1002/tcr.202000060.

[27] C. Li *et al.*, "A self-adhesive, self-healing and antibacterial hydrogel based on PVA/MXene-Ag/sucrose for fast-response, high-sensitivity and ultra-durable strain sensors," *New Journal of Chemistry*, vol. 47, no. 14, pp. 6621–6630, 2023, doi: 10.1039/D3NJ00586K.

[28] Y. Zhang *et al.*, "Tough hydrogels with tunable soft and wet interfacial adhesion," *Polym Test*, vol. 93, p. 106976, Jan. 2021, doi: 10.1016/j.polymertesting.2020.106976.

[29] I. Cunha *et al.*, "Reusable Cellulose-Based Hydrogel Sticker Film Applied as Gate Dielectric in Paper Electrolyte-Gated Transistors," *Adv Funct Mater*, vol. 27, no. 16, Apr. 2017, doi: 10.1002/adfm.201606755.